

pubs.acs.org/JPCC Article

# Thermodynamics of Carbon Monoxide Adsorption on Cu/SBA-15 Catalysts: Under Vacuum versus under Atmospheric Pressures

Published as part of The Journal of Physical Chemistry virtual special issue "Cynthia Friend Festschrift". Tongxin Han, Ilkeun Lee, Yueqiang Cao, Xinggui Zhou, and Francisco Zaera\*



Cite This: J. Phys. Chem. C 2022, 126, 3078-3086

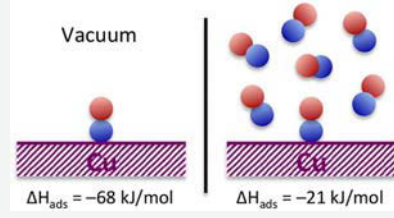


**ACCESS** I

Metrics & More

Article Recommendations

ABSTRACT: The thermodynamics of the adsorption of carbon monoxide on a copperbased catalyst were estimated by using data from in situ infrared absorption spectroscopy experiments. A direct comparison was performed between the energetics under a vacuum environment versus in the presence of CO gas. It was found that the magnitude of the enthalpy of adsorption is reduced by almost a factor of 4 in going from the first case to the second, from  $\Delta H^{\circ}_{ads,vacuum} = -82 \text{ kJ/mol}$  to  $\Delta H^{\circ}_{ads,CO-atm} = -21 \text{ kJ/mol}$ . Furthermore, isosteric analysis of the data indicated that the magnitude of the latter decreases in the low-coverage limit, to values below  $\Delta H^{\circ}_{ads,CO-atm} = -18$  kJ/mol, a trend opposite to what has been reported in other systems. These observations are explained in terms of the



associated standard entropy of adsorption, which in the presence of gas-phase CO was estimated at  $\Delta S^{\circ}_{ads,CO-atm} \sim -24 \, J/(mol \, K)$ , a value much smaller in magnitude than the standard entropy of CO condensation. The excess entropy of CO adsorption over that of CO condensation is here ascribed to excess entropy in the adsorbed state due to additional phenomena induced by the gas-phase molecules such as adsorbate displacement and adsorbate-assisted adsorption steps.

## 1. INTRODUCTION

Virtually all chemical reactions promoted by solids start with the adsorption of the reactants on the surface of the catalytic phase and end with the desorption of the products. In fact, in many cases those steps may determine the kinetics of the overall process. Yet, information about their thermodynamics and kinetics under realistic reaction conditions is still limited. Basic information about the energetics of the bonding of adsorbates to surfaces has been acquired in recent decades with the help of modern surface science techniques, in particular temperature-programmed desorption (TPD) and, more recently, also with the aid of quantum mechanics calculations. Invaluable as the resulting knowledge has been, the energetics acquired this way usually refers to the uptake of molecules on surfaces under vacuum and often in the low-coverage limit. It is well-known that increasing coverages, as expected when in the presence of gases or a liquid phase, quite often leads to a drastic reduction in adsorption energy. Additional effects on the adsorption-desorption process are also expected to be introduced by the gas or liquid phase itself, although this has not been discussed in the literature in much detail; in general, studies of adsorption kinetics and thermodynamics in situ in the presence of reactants remain somewhat scarce.<sup>2,3</sup> Here, we estimate the enthalpy and the entropy of the adsorption of carbon monoxide on copper catalysts, with emphasis on contrasting the behavior of this system under vacuum versus in the presence of the adsorbing gas. Carbon monoxide is a reactant in many major catalytic processes and a common

prototypical adsorbate, and copper catalysts are used for the hydrogenation of CO to methanol<sup>4–8</sup> and the low-temperature promotion of the water-shift reaction, 9-11 among other processes. When a second transition metal is added in small amounts, to form so-called single-atom alloys (SAA), 12 copper can also be used as a selective catalyst for other reactions, for the hydrogenation of organic reactants with multiple double or triple bonds, for instance. 13-18 This latter application has been the motivation behind this study. 19,20

We found that, indeed, the thermodynamics of CO adsorption on copper are quite different under vacuum versus in the presence of the gas phase. In particular, the magnitudes of both the enthalpy and the entropy of adsorption are reduced drastically upon the addition of gas-phase CO. We interpret these changes as the result of the incorporation of new steps by the free molecules, including adsorbate displacement and adsorbate-assisted adsorption. We contend that the changes seen here and the explanation provided may be quite general and apply to many reversible adsorption processes.

Received: December 20, 2021 January 24, 2022 Published: February 4, 2022





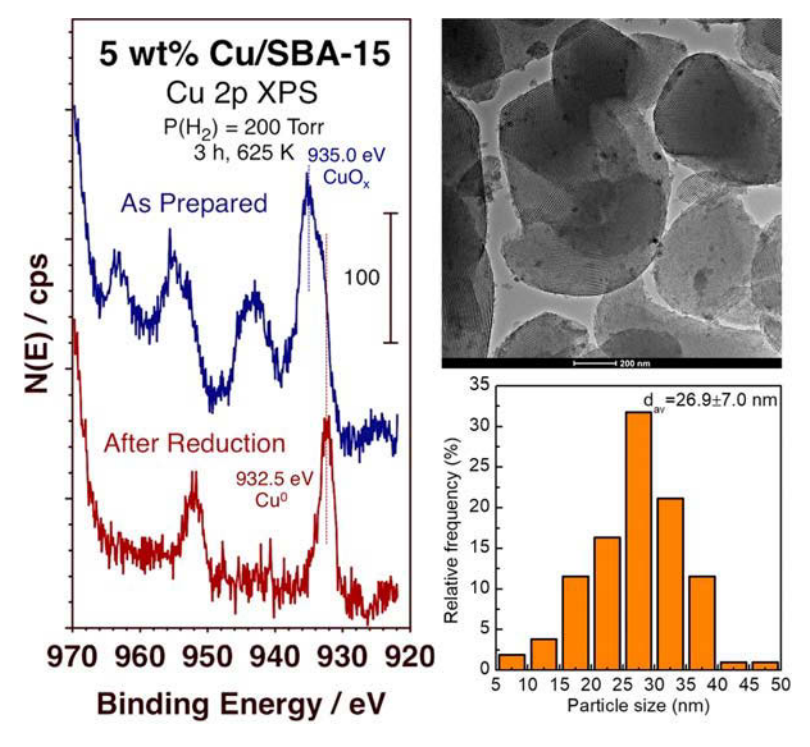
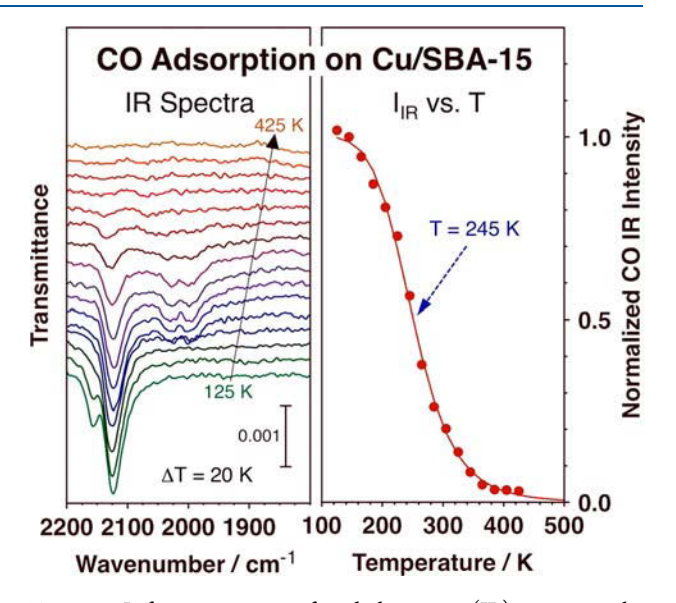


Figure 1. Left: Cu 2p XPS spectra for our Cu/SBA-15 catalyst, obtained before and after reduction. Right: TEM image and Cu NP size distribution.

## 2. METHODS

The in situ infrared absorption spectroscopy (IR) studies reported below were performed in a transmission IR cell reported in previous publications, <sup>21–24</sup> a standard setup similar to that seen in many other laboratories. <sup>25–30</sup> The catalyst, a 5 wt % Cu/SBA-15 solid, was prepared by incipient wetness impregnation (using copper nitrate)19 and made into a pellet that was placed in the center of the IR cell and pretreated before use by exposing it to a H<sub>2</sub> atmosphere (200 Torr) at 625 K for 3 h. Figure 1 provides some characterization results for this catalyst: the left panel shows Cu 2p X-ray photoelectron spectroscopy (XPS) data attesting to the fully reduced state of the Cu nanoparticles (NPs) after the H<sub>2</sub> pretreatment, whereas the right section displays a typical transmission electron microscopy (TEM) image of the catalyst and the particle size distribution estimated from several of such images ( $\langle d \rangle \sim 27$  nm). For the experiments involving an equilibrium with gas-phase CO, the IR cell was filled with the desired pressure of carbon monoxide and the IR spectra were recorded in situ in the presence of the gas as the sample was heated and cooled to evaluate the temperature dependence of the adsorption equilibrium; three cycles were performed to corroborate that the CO surface coverages measured by the IR peaks correspond to equilibrium states. In the case of the lowtemperature adsorption measurements under vacuum, the catalyst was exposed to 50 Torr of CO for 0.5 h, after which the cell was evacuated for 10 min and the IR spectra were recorded from 125 to 475 K at 20 K intervals as the sample and cell were warmed up. It should be indicated that, although the vacuum used in these experiments was that reached with a mechanical pump ( $P_{\rm bkg} \sim 1 \times 10^{-2}$  Torr), the residual gas was composed mainly of water (and some oil from the pump); the CO partial pressure was negligible, as indicated by the fact that, in experiments such as those in Figure 2, no CO uptake was



**Figure 2.** Left: transmission infrared absorption (IR) spectra in the C–O stretching region for CO adsorbed on a 5 wt % Cu/SBA-15 catalyst as a function of temperature during heating under vacuum, after initial adsorption at 125 K in 50 Torr CO. Right: normalized peak intensity for the main feature in the IR spectra at 2124 cm<sup>-1</sup> due to CO adsorption on Cu as a function of temperature, together with a fit to a sigmoidal curve.

seen within the time frame of the IR runs after cooling the sample to 125 K, a temperature where the sticking coefficient of CO is close to unity. Only when CO was added to the cell (pressures as low as 0.1 Torr were explored) was CO uptake on the catalyst seen. All spectra were acquired with a resolution of 2 cm<sup>-1</sup> by averaging the data from 16 scans, and corrected

by using background spectra obtained under the same condition before adsorption. CO surface coverages were estimated by integration of the areas of the IR peaks, and reported in monolayers (ML) relative to the estimated saturation coverage (set to  $\theta_{\rm CO,sat}=1$  ML). Note that saturation under atmospheric CO pressures was estimated to be  $\sim \! 30\%$  higher than under vacuum ( $\theta_{\rm CO,sat,vacuum}$ ).

## 3. RESULTS

The desorption of adsorbed carbon monoxide on the Cu/SBA-15 catalyst was first probed as a function of temperature under vacuum. The corresponding infrared absorption spectroscopy data are shown in Figure 2. The main peak seen at 2124 cm<sup>-1</sup>, visible from 125 to ~350 K, is assigned to CO adsorption on metallic Cu atop site on the basis of previous reports;<sup>31–35</sup> a brief discussion of this assignment is provided later. At low temperatures, below 150 K, an additional feature is detected on the high-frequency side (at ~2160 cm<sup>-1</sup>), most likely from adsorption of CO on oxidized copper sites (the lower desorption temperature seen for this species indicates weaker CO bonding to CuO<sub>x</sub>), and a weaker broad double feature is also seen in the 1950-2050 cm<sup>-1</sup> range at intermediate temperatures (205-325 K), the origin of which we do not understand at the present time. Focusing on the CO bonded to metallic copper, the intensity of the peak was followed versus annealing temperature to extract information about the energetics of the adsorption (Figure 2, right panel). It was determined that the desorption rate reaches a maximum value at ~245 K, a result roughly consistent with that seen in temperature-programmed desorption (TPD) experiments on Cu single crystals once the differences in heating rate, gas load, and pumping speed are taken into account. By use of Redhead's analysis,  $^{36}$  an estimated value of  $A = 1 \times 10^{15} \text{ s}^{-1}$ for the preexponential factor, and a heating rate of 20 K in 10 min, the activation energy for CO desorption from this Cu/ SBA-15 catalyst, which can also be associated with the enthalpy of adsorption, is estimated to be  $E_{\rm a} \sim -\Delta H^{\circ}_{\rm ads,vacuum}$  = 82 kJ/ mol, a value in the range of what has been reported in the past for stepped Cu single crystals.<sup>37</sup> It should be emphasized that this is an approximate value, however, as it assumes a constant adsorption energy as a function of coverage, which may not be the case. Nevertheless, the maximum adsorption rate used in our calculations corresponds to approximately half surface saturation, and the most acute changes in desorption energies for CO have been reported at higher coverages, close to a full monolayer.<sup>38</sup> We contend that within the margin of error of these measurements our desorption energy estimate is representative of the adsorption energetics of CO on the Cu catalyst under vacuum over most of the coverage range.

Next, CO adsorption was probed *in situ* in the presence of a CO atmosphere (after two reduction cycles by heating to 495 K and cooling back down to 300 K in CO). Typical IR data recorded in those experiments are shown in Figure 3: the left panel shows the C-O stretching region for both the catalyst in the presence of the gas (dark traces, 50 Torr in this case) and the blank experiments with CO gas only, with the catalyst pellet removed (light traces). The gas-phase molecules are clearly detected, seen as the expected two broad features between 2000 and 2250 cm<sup>-1</sup> due to the different rotational levels within the main the C-O stretching vibrational mode. Nevertheless, an additional signal, in the form of a sharper peak at about 2124 cm<sup>-1</sup>, is visible in these spectra assignable to CO

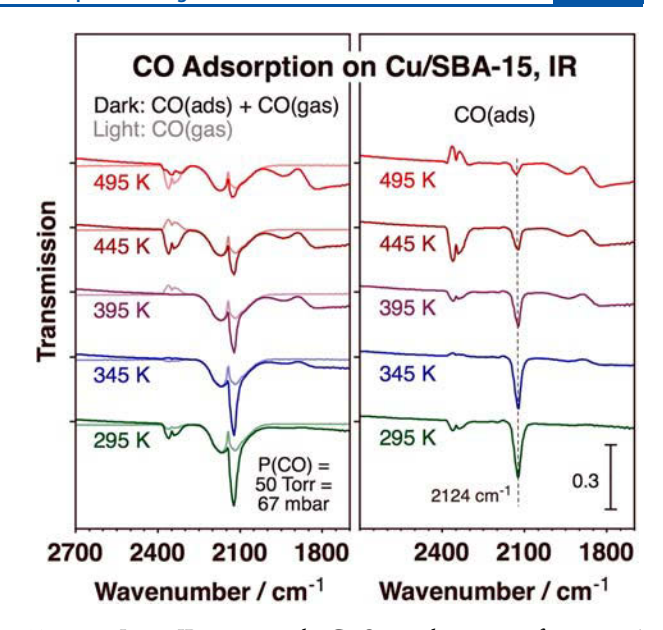


**Figure 3.** *In situ* IR spectra in the C–O stretching region for a 5 wt % Cu/SBA-15 catalyst exposed to 50 Torr (67 mbar) of carbon monoxide as a function of catalyst temperature. Left: raw data recorded in the presence of the gas-phase CO (dark traces), together with reference spectra obtained in the absence of the catalyst, for the gas alone (light traces). Right: spectra for the adsorbed CO, obtained via subtraction of the corresponding traces shown in the right panel. The peak highlighted at 2124 cm<sup>-1</sup> corresponds to CO adsorbed on atop sites on the surface of the metallic copper NPs.

adsorbed on Cu. The right panel of Figure 3 displays the same spectra after subtracting the gas-phase contribution: a clear peak remains at  $2124~\rm cm^{-1}$  corresponding to CO bonded on atop sites on the surface of the metallic Cu NPs of the catalyst. The peaks in the  $2300-2400~\rm cm^{-1}$  region correspond to gas-phase CO<sub>2</sub>, from both incomplete purging of the IR beam path (ambient air contains some CO<sub>2</sub>) and oxidation of CO (see below).

The adsorption of CO reported in Figure 3 is reversible. To confirm this, repeated heating and cooling cycles were performed in situ in the presence of the same CO gas atmosphere. The resulting data are exemplified by the plots reported in Figure 4, with 100 Torr of CO in that case. It should be noted that initial CO adsorption at room temperature was minimal (bottom trace in left panel of Figure 4); in spite of the in situ H<sub>2</sub> pretreatment performed before the use of the catalyst, it appears that the Cu nanoparticles retain a thin oxide layer that prevents binding of the adsorbate. Luckily, CO is itself a strong reducing agent that helps remove such oxide layer, so a significant increase in CO uptake is seen in the first heating cycle as a temperature of 495 K is reached, in conjunction with the generation of CO2 gas produced by CO oxidation with the oxygen atoms of the oxidized Cu surface (Figure 4, left panel). After that sequence of events, it can be seen from Figure 4 that the IR peak associated with CO bonded to metallic Cu increases and decreases in size reversibly as subsequent cooling and heating cycles are followed. The peak intensities measured at any of the given temperatures are quite similar in all cases, evidencing the reversibility of the process.

Data such as those reported in Figures 3 and 4 were analyzed to develop isothermal curves of CO surface coverage

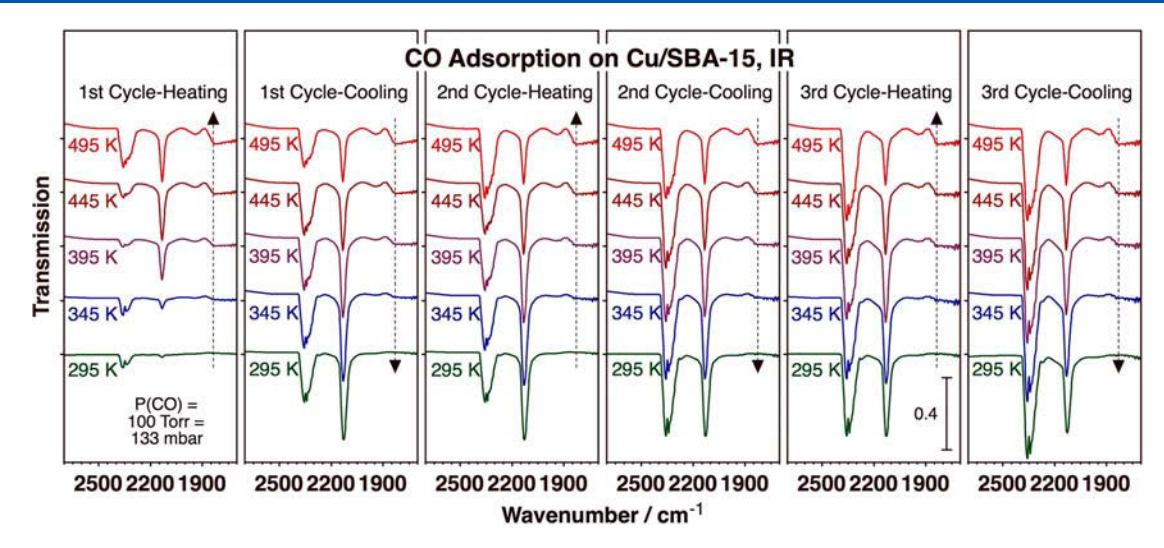
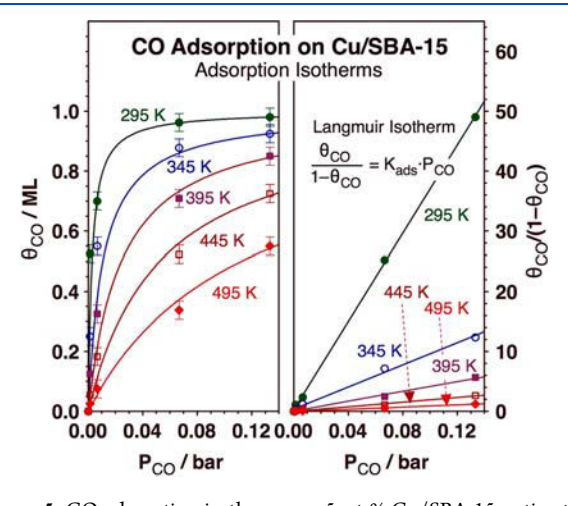


Figure 4. In situ IR spectra in the C-O stretching region for a 5 wt % Cu/SBA-15 catalyst exposed to 100 Torr (133 mbar) of carbon monoxide as a function of catalyst temperature. Shown are the data for three consecutive heating and cooling cycles to highlight the reversibility of the adsorption.

 $(\theta_{\rm CO})$  on the Cu/SBA-15 catalyst as a function of CO pressure  $(P_{\rm CO})$ . The results are shown in Figure 5: the symbols



**Figure 5.** CO adsorption isotherms on 5 wt % Cu/SBA-15, estimated from the intensity of the IR peaks in data such as those shown in Figures 3 and 4. The data are displayed both in their basic form, as CO coverage versus CO pressure (left), and in linearized form, by using the Langmuir isotherm formulation (right).

correspond to the experimental values, whereas the solid lines are the best fits to the Langmuir isotherm equation. The data are plotted in two modes: in the original  $\theta_{\rm CO}$  versus  $P_{\rm CO}$  form (left panel), and in a linearized form to help extract the corresponding adsorption equilibrium constants ( $K_{\rm ads}$ ). The latter were then plotted in van't Hoff mode, that is, as  $\ln(K^{\rm o}_{\rm ads})$  =  $\ln(K_{\rm ads}P^{\rm o}_{\rm CO})$  versus 1/T, to extract the appropriate thermodynamic parameters (Figure 6). In these calculations (and all subsequent ones), the thermodynamic standard states were taken as  $P^{\rm o}_{\rm CO} = 1$  bar,  $\theta^{\rm o}_{\rm CO} = 0.5$  ML, and  $\theta^{\rm o}_{\rm empty} = 1 - \theta^{\rm o}_{\rm CO} = 0.5$  ML, as typically used in cases where the adsorbates are presumed to be immobile.  $^{39,40}_{\rm o}$  As indicated in Figure 6, values of  $\Delta H^{\rm o}_{\rm ads,CO-atm} = -21.3$  kJ/mol and  $\Delta S^{\rm o}_{\rm ads,CO-atm} = -23.7$  J/(mol K) were estimated from this analysis.

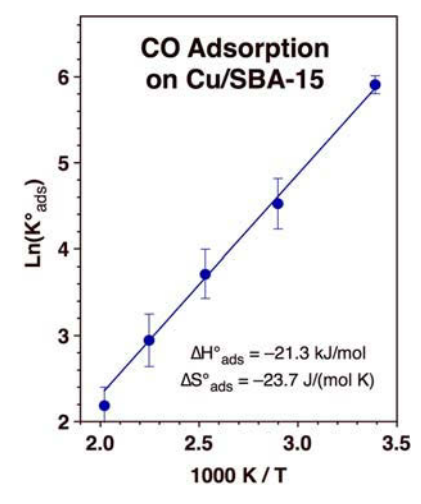


**Figure 6.** Van't Hoff plot of the standard equilibrium constants for the adsorption of CO on 5 wt % Cu/SBA-15 ( $K^{\circ}_{ads}$ , from the slope in the traces in the right panel of Figure 5) as a function of temperature, from which the values for the standard enthalpy and the standard entropy of adsorption were extracted.

Two issues need to be considered when interpreting the thermodynamic data reported above. First, the intensity of the IR peak due to the adsorbed CO is in many cases not linearly dependent on the surface coverage of the adsorbate, as it has implicitly been assumed here. Instead, that intensity tends to grow at a lesser rate in the high coverage range because of intermolecular dipole-dipole and other interactions<sup>41-</sup> However, the effect is less pronounced with supported metal nanoparticles because of the higher degree of disorder involved, and may not play a significant role here. Second, because of those interadsorbate interactions, the adsorption energy of CO on metals tends to change with surface coverage, typically dropping considerably close to monolayer saturation. To check on these potential dependences of adsorption energy on coverage, an alternative isosteric analysis of the data was performed in the limit of low coverages. For that, the pressures of CO required to reach a certain pre-established coverage

were estimated via linear interpolation of the experimental data (a linear dependence is expected in the low-coverage limit on the basis of the Langmuir isotherm equation), and plotted versus temperature in linearized form (as  $\ln(P_{\rm CO})$  vs 1/T). The left panel of Figure 7 shows the resulting isosters for  $\theta_{\rm CO}$  =

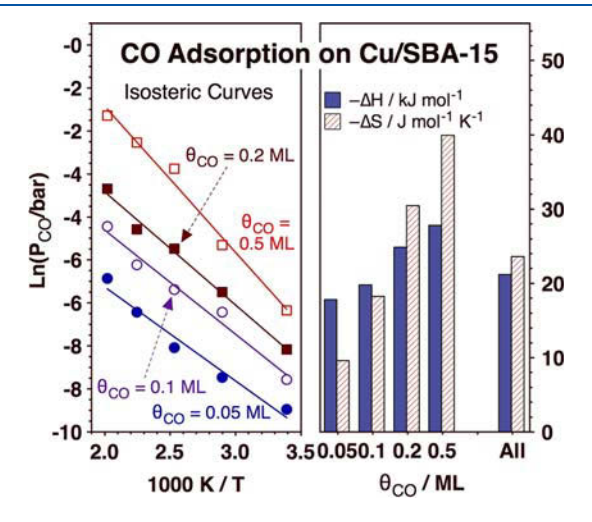


**Figure 7.** Left: isosteric plots of CO pressure vs temperature, in Van't Hoff form, for four values of the CO coverage ( $\theta_{\rm CO} = 0.05, \, 0.1, \, 0.2, \,$  and 0.5 ML). Right: standard enthalpy and standard entropy of adsorption estimated from the plots in the left panel.

0.05, 0.1, 0.2, and 0.5 ML, and the right panel shows the thermodynamic parameters calculated from that analysis. For  $\theta_{\rm CO}=0.5$  ML, the enthalpy of adsorption is estimated at  $\Delta H_{\rm ads,CO-atm}(\theta_{\rm CO}=0.5$  ML)  $\sim -28$  kJ/mol, much smaller in magnitude than that reported above for the same coverage under vacuum,  $\Delta H_{\rm ads,vacuum}(\theta_{\rm CO}=0.5$  ML)  $\sim -82$  kJ/mol. Interestingly, it was found that the magnitudes of both the enthalpy and the entropy of the adsorption are lower, not higher as usually reported, at low coverages (Figure 7, right). A third possible approach to analyze the CO adsorption data is in isobaric form. The corresponding plots of  $\ln[\theta_{\rm CO}/(1-\theta_{\rm CO})]$  vs 1/T are displayed in Figure 8. Values of  $\Delta H^{\circ}_{\rm ads,CO-atm}=-21.9\pm2.0$  kJ/mol and  $\Delta S^{\circ}_{\rm ads,CO-atm}=-22.8\pm6.0$  J/(mol K) were estimated from the slopes of that figure.

## 4. DISCUSSION

In this section, we start by briefly discussing our assignment of the main IR band at 2124 cm<sup>-1</sup> seen in the spectra reported above to CO adsorbed on atop sites of metallic Cu, as there has been some discussion in the literature about such assignment, which is not straightforward. <sup>34,44</sup> Certainly, the C–O stretching frequency of carbon monoxide adsorbed on atop sites of copper single-crystal surfaces is typically below 2100 cm<sup>-1</sup>; <sup>44–48</sup> features in the spectra at higher frequencies have been assigned to CO bonding to oxidized Cu atoms. <sup>32,49</sup> Nevertheless, higher frequencies have also been seen on stepped and kinked metallic Cu surfaces <sup>50</sup> and also on supported Cu catalysts. <sup>31–34,51,52</sup> It has been reported that CO adsorption on catalysts with larger Cu NPs tends to exhibit higher C–O stretching frequencies as well; <sup>32</sup> in that context, the high value reported here is consistent with the fact that the average NP diameter of our catalyst is  $\langle d \rangle \sim 27$  nm. We put forward two main arguments for why we believe that the peak seen at 2124 cm<sup>-1</sup> in our data corresponds to adsorption on

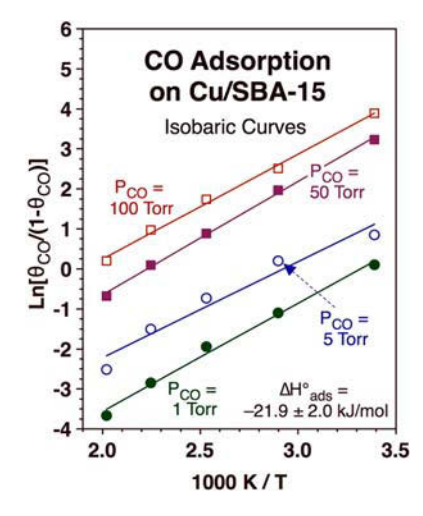


**Figure 8.** Isobaric plots of CO coverage versus temperature, in Van't Hoff form, for several CO pressures ( $P_{CO} = 1, 5, 50$ , and 100 Torr).

metallic copper. First, we are confident that our catalyst is fully reduced in the experiments performed in the presence of a CO atmosphere. The catalyst was always pretreated in H2 in situ before each experiment, and the Cu 2p XPS data provided in Figure 1 indicate that such treatment leads to the full reduction of the Cu NPs. It could be argued that sometimes the addition of an atmosphere of reacting gases may lead to the formation of a thin layer of an oxide, but carbon monoxide is itself an excellent reducing agent, and the data in Figure 4 show that, indeed, CO is capable of removing any remaining oxygen from the Cu surface upon heating to high (495 K) temperatures; witness the formation of gas-phase carbon dioxide, as indicated by the IR features in the 2300-2400 cm<sup>-1</sup> range, and the subsequent increase in CO uptake on the surface. Our second argument relates to the thermal stability of the adsorbed CO under vacuum, as indicated by the data in Figure 2: the CO associated with the 2124 cm<sup>-1</sup> peak remains bounded to the catalyst until ~245 K, whereas the second feature seen at 2160 cm<sup>-1</sup>, identified with the weaker adsorption on oxidized Cu, goes away by 150 K.

The adsorption energetics of CO on the Cu/SBA-15 catalyst was first probed under vacuum by performing a temperatureprogrammed experiment using IR for surface coverage determination. The data in Figure 2 indicate that the CO desorption rate peaks at about 245 K, which corresponds to an adsorption enthalpy of approximately  $\Delta H_{\text{ads,vacuum}} = -82 \text{ kJ/}$ mol. This value is consistent with results obtained in the past with single crystals (Table 1), with the caveat that the CO adsorption energy is highly dependent on both surface coverage and surface structure. For instance, a value of  $E_{\rm des}(\theta_{\rm CO} \rightarrow 0 \text{ ML}) \sim -\Delta H_{\rm ads,vacuum} = 84 \text{ kJ/mol has been}$ reported for the zero-coverage limit of the adsorption of CO on the atop step-edge sites of Cu(410), but that number is reduced to  $E_{\rm des}(\theta_{\rm CO}=0.5~{\rm ML})\sim70~{\rm kJ/mol}$  at half saturation.<sup>37</sup> Earlier reported data are also in the appropriate energy range, albeit with lower values for flat terraces:  $E_{\text{des}}(\theta_{\text{CO}})$  $\leq$  0.5 ML)  $\sim$  50–55 kJ/mol was reported for both CO/Cu(111)  $^{53}$  and CO/Cu(110)  $^{54}$  for coverages below halfsaturation, and CO desorption from the steps in defective Cu(110) peaks at 205 K, a temperature equivalent to  $E_{\rm des} \sim 60$ kJ/mol.<sup>50</sup> The lower CO desorption energies reported for the basal planes of single crystals suggest that the adsorption on

Table 1. Selected Reported Values for the Enthalpy of Adsorption of CO on Copper Surfaces

surface	$\Delta H_{ m ads} \  m (kJ/mol)$	method	comment	ref
UHV				
Cu(111)	−49 to −53	surface potential	independent of coverage	53
Cu(110)	−51 to −54	TPD	slight increase up to $\theta_{\rm CO} \sim 0.3$ ML, then abrupt drop to $-42$ kJ/mol	54
Cu(410)	−84 to −65	TPD	progressively decreasing with coverage	37
Cu/SiO <sub>2</sub>	-82	IR		this work
CO atmosphere				
Cu/SiO <sub>2</sub>	−48 to −22	IR	increases in magnitude with increasing nanoparticle size, all converge to -22 kJ/mol at saturation	32
Cu/SiO <sub>2</sub>	-20	IR	higher adsorption energies on Cu <sup>+</sup> and Cu <sup>2+</sup> sites	33
Cu/Al <sub>2</sub> O <sub>3</sub>	-18	IR		33
Cu/ diamond	-21	IR		33
Cu/SBA- 15	-21	IR		this work

supported metal NPs may be dominated by binding to low-coordination sites in edges, kinks, and other structural defects.

The equilibrium enthalpy of adsorption for CO on Cu/SBA-15 under an atmosphere of gas-phase CO turns out to be much lower in magnitude. Indeed, the isothermal adsorption data reported in Figures 5 and 6 yielded an adsorption enthalpy value of  $\Delta H_{\rm ads,CO-atm} = -21.3$  kJ/mol, about a fourth of the value measured under vacuum. It could be argued that the difference originates from differences in surface coverage, but the isosteric analysis reported in Figure 7 indicates that this is not the case; if anything, the magnitude of the adsorption enthalpy decreases somewhat when approaching the low CO coverage limit. The isobaric plot in Figure 8 further confirms these results.

It may be worth asking if the  $\Delta H_{ads}$  values obtained here for CO adsorption on Cu/SBA-15 in the presence of gas-phase CO make sense. Unfortunately, because of the weak adsorption energies involved, attempts to detect reversibly bonded CO on Cu under a CO atmosphere with model systems, on Cu single-crystal surfaces and by using modern surface-science instrumentation, have not been successful; both infrared absorption (IR)<sup>48</sup> and atmospheric-pressure X-ray photoelectron spectroscopy (AP-XPS)<sup>5,5</sup> experiments with Ptdoped Cu could only reach CO pressures of up to 0.1 Torr and could therefore only detect the CO bonded to Pt sites. On the other hand, a couple of early reports on CO adsorption on supported Cu catalysts (Table 1) are consistent with our results. Using Cu/SiO<sub>2</sub> catalysts, Kohler and co-workers reported heats of adsorption on metallic copper surfaces approaching a value of  $\Delta H_{\rm ads,CO-atm} \sim -22$  kJ/mol at coverages close to saturation,<sup>32</sup> essentially the same as what we have measured here. They did also report a CO coverage dependence of that parameter, with higher magnitudes for the adsorption energy at lower coverages (a trend opposite to that seeing by us in Figure 7), but this effect was the most pronounced with catalysts with high Cu loadings (>6 wt %) and minimal for Cu loadings below 4 wt %. In a more recent report, Dandekar et al. reported  $\Delta H_{\rm ads,CO-atm} = -20.1 \ {\rm kJ/mol}$ for CO adsorption on the metallic sites of a 5.1 wt % Cu/SiO<sub>2</sub> catalyst, <sup>33</sup> again in good agreement with our results. It does appear that the severe reduction in CO adsorption energy observed on Cu catalysts when transitioning from a vacuum to an atmosphere of CO is real.

What remains to be discussed is an explanation for the difference. Certainly, the thermodynamic values reported here are only approximate, as they exhibit large errors due to the fact that they do not include coverage effects or the potential of the existence of different adsorption sites within the Cu NPs of the catalyst. However, the range of values for the enthalpy of adsorption of CO on Cu under vacuum ( $\Delta H_{\rm ads,vacuum} \sim -85$  to −50 kJ/mol) reported by us and others does not overlap at all with that corresponding to adsorption under a CO gas atmosphere ( $\Delta H_{\rm ads,CO-atm} \sim -45$  to -20 kJ/mol) (Table 1), regardless of CO surface coverage; that alone cannot explain the large difference in the energetics seen in both cases. Instead, we take a look at the entropy of the adsorption processes, which has not been reported previously but that we were able to extract from our data: values of  $\Delta S^{\circ}_{ads,CO-atm}$  = -23.7 and -22.8 J/(mol K) were obtained from the isothermal and isobaric analysis in Figures 6 and 8, respectively. For comparison, the standard entropy of CO vaporization (the negative of the standard entropy of condensation) at the boiling point of CO ( $T_b^\circ = 81.6 \text{ K}$ ) is  $-\Delta S^\circ_{\text{vap},81.6\text{K}} = \Delta S^\circ_{\text{cond},81.6\text{K}} = -74 \text{ J/(mol K)}.^{56}$  If we assume that the liquid remains fully frozen and that only the heat capacity of CO gas contributes to the change in entropy of vaporization when transitioning from the boiling point to room temperature (admittedly an extreme approximation), the standard entropy of vaporization at room temperature is estimated as  $-\Delta S^{\circ}_{\text{vap,298K}} = \Delta S^{\circ}_{\text{cond,298K}} \le -111 \text{ J/(mol K).}^{56}$ The fact that the magnitude of the adsorption entropy determined in our studies is so much lower than that for the CO condensation indicates that there is an entropy deficit in the former process beyond that related to immobilization of CO molecules on the surface. Stated a different way, the entropy of the adsorbed CO is larger than that expected for CO fully anchored on the solid surface. We suggest that such excess may reflect a certain degree of 2D mobility of the adsorbed CO within the surface, perhaps because of a relatively low barrier for surface diffusion.<sup>57</sup> In that context, it is interesting to note that, according to the data in Figure 7, the magnitude of the adsorption entropy decreases significantly at low coverages, presumably because there is more room on the surface for the few CO molecules on the surface to diffuse around without hindrance by other adsorbates. It is also possible that additional entropy is introduced by the presence of gas-phase CO because of adsorbate displacements by incoming molecules<sup>58-60</sup> and/or adsorbate-assisted desorption<sup>61–64</sup> steps, as seen in other systems. Both these processes can add degrees of disorder, and hence entropy, to the COcovered surface. Note that the same argument does not hold for CO desorption in vacuum environments: according to transition state theory, a pre-exponential factor of  $A = 1 \times 10^{15}$ s<sup>-1</sup> for that process (as typically assumed) amounts to an increase in entropy upon desorption at room temperature of  $\Delta S_{\text{des},298K}^{\ddagger} = 43 \text{ J/(mol K)}$ , and if the value of  $A = 1 \times 10^{19} \text{ s}^{-1}$ reported by Kokaji et al. for CO desorption from Cu(410) is used,  $\Delta S^{\ddagger}_{\text{des},298\text{K}} \sim 120 \text{ J/(mol K)}$ . Clearly, low desorption entropies appear to be unique to the release of adsorbed CO from the Cu surface into the gas phase under atmospheric pressures of the adsorbing gas. This difference may explain the large reductions in desorption enthalpies seen in going from

vacuum to atmospheric pressures, and it is likely to be general, not only applicable to the case of CO adsorption on Cu/SBA-15 but also to most reversible adsorption processes. Finally, it is worth mentioning that the simultaneous changes in enthalpies and entropies that yield similar equilibrium or kinetic constants for a family of related reactions or for varying reaction conditions (as is the case here) has been observed before and characterized as a "compensation effect"; several explanations have been offered for such an effect.

## 5. CONCLUSIONS

In this study, the thermodynamics of the adsorption of CO on the metal surface of a Cu/SBA-15 catalyst was contrasted in two different environments: under vacuum versus in the presence of atmospheric pressures of CO. Interestingly, marked differences were seen. Specifically, the enthalpy of adsorption was estimated to vary from  $\Delta H^{\circ}_{\rm ads,vacuum} = -82~{\rm kJ/mol}$  to  $\Delta H^{\circ}_{\rm ads,CO-atm} \sim -21~{\rm kJ/mol}$ . This difference is too large to be explained by coverage effects alone, especially since the isosteric calculations in the low CO surface coverage limit indicated that the enthalpy of CO adsorption actually decreases (instead of increasing, as seen in many other systems) as the coverage decreases. Instead, we explain the change on the basis of entropic effects introduced by the presence of CO gas such as adsorbate displacement and adsorbate-assisted adsorption steps.

## AUTHOR INFORMATION

### **Corresponding Author**

Francisco Zaera — Department of Chemistry and UCR Center for Catalysis, University of California, Riverside, Riverside, California 92521, United States; orcid.org/0000-0002-0128-7221; Email: zaera@ucr.edu

# Authors

Tongxin Han – Department of Chemistry and UCR Center for Catalysis, University of California, Riverside, Riverside, California 92521, United States

Ilkeun Lee – Department of Chemistry and UCR Center for Catalysis, University of California, Riverside, Riverside, California 92521, United States

Yueqiang Cao — State Key Laboratory of Chemical Engineering, School of Chemical Engineering, East China University of Science and Technology, Shanghai 200237, China; Oorcid.org/0000-0002-1036-4049

Xinggui Zhou — State Key Laboratory of Chemical Engineering, School of Chemical Engineering, East China University of Science and Technology, Shanghai 200237, China; orcid.org/0000-0002-4736-3672

Complete contact information is available at: https://pubs.acs.org/10.1021/acs.jpcc.1c10722

#### Notes

The authors declare no competing financial interest.

# **■** ACKNOWLEDGMENTS

Financial support for this project was provided by a grant from the U.S. National Science Foundation, Division of Chemistry (Grant NSF-CHE1953843).

## REFERENCES

(1) Schumacher, N.; Boisen, A.; Dahl, S.; Gokhale, A. A.; Kandoi, S.; Grabow, L. C.; Dumesic, J. A.; Mavrikakis, M.; Chorkendorff, I.

- Trends in Low-Temperature Water-Gas Shift Reactivity on Transition Metals. *J. Catal.* **2005**, 229, 265-275.
- (2) Davies, J. C.; Nielsen, R. M.; Thomsen, L. B.; Chorkendorff, I.; Logadóttir, Á.; Lodziana, Z.; Nørskov, J. K.; Li, W. X.; Hammer, B.; Longwitz, S. R.; et al. CO Desorption Rate Dependence on CO Partial Pressure over Platinum Fuel Cell Catalysts. *Fuel Cells* **2004**, *4*, 309–319.
- (3) Johansson, M.; Lytken, O.; Chorkendorff, I. The Sticking Probability for  $H_2$  on Some Transition Metals at a Hydrogen Pressure of 1 bar. *J. Chem. Phys.* **2008**, 128, 034706.
- (4) Nix, R. M.; Rayment, T.; Lambert, R. M.; Jennings, J. R.; Owen, G. An in Situ X-Ray Diffraction Study of the Activation and Performance of Methanol Synthesis Catalysts Derived from Rare Earth-Copper Alloys. *J. Catal.* 1987, 106, 216–234.
- (5) Nerlov, J.; Sckerl, S.; Wambach, J.; Chorkendorff, I. Methanol Synthesis from CO<sub>2</sub>, CO and H<sub>2</sub> over Cu(100) and Cu(100) Modified by Ni and Co. *Appl. Catal., A* **2000**, *191*, 97–109.
- (6) Yang, R. Q.; Gai, X. K.; Xing, C.; Mao, J. W.; Lv, C. X. Performance of Cu-Based Catalysts in Low-Temperature Methanol Synthesis. *Adv. Mater. Res.* **2014**, 1004–1005, 1623–1626.
- (7) van de Water, L. G. A.; Wilkinson, S. K.; Smith, R. A. P.; Watson, M. J. Understanding Methanol Synthesis from CO/H<sub>2</sub> Feeds over Cu/CeO<sub>2</sub> Catalysts. *J. Catal.* **2018**, *364*, 57–68.
- (8) Zhu, J.; Su, Y.; Chai, J.; Muravev, V.; Kosinov, N.; Hensen, E. J. M. Mechanism and Nature of Active Sites for Methanol Synthesis from CO/CO<sub>2</sub> on Cu/CeO<sub>2</sub>. ACS Catal. **2020**, 10, 11532–11544.
- (9) Li, Y.; Fu, Q.; Flytzani-Stephanopoulos, M. Low-Temperature Water-Gas Shift Reaction over Cu- and Ni-Loaded Cerium Oxide Catalysts. *Appl. Catal., B* **2000**, *27*, 179–191.
- (10) Gawande, M. B.; Goswami, A.; Felpin, F.-X.; Asefa, T.; Huang, X.; Silva, R.; Zou, X.; Zboril, R.; Varma, R. S. Cu and Cu-Based Nanoparticles: Synthesis and Applications in Catalysis. *Chem. Rev.* **2016**, *116*, 3722–3811.
- (11) Chen, A.; Yu, X.; Zhou, Y.; Miao, S.; Li, Y.; Kuld, S.; Sehested, J.; Liu, J.; Aoki, T.; Hong, S.; et al. Structure of the Catalytically Active Copper—Ceria Interfacial Perimeter. *Nat. Catal.* **2019**, *2*, 334—341.
- (12) Hannagan, R. T.; Giannakakis, G.; Flytzani-Stephanopoulos, M.; Sykes, E. C. H. Single-Atom Alloy Catalysis. *Chem. Rev.* **2020**, 120, 12044–12088.
- (13) Kyriakou, G.; Boucher, M. B.; Jewell, A. D.; Lewis, E. A.; Lawton, T. J.; Baber, A. E.; Tierney, H. L.; Flytzani-Stephanopoulos, M.; Sykes, E. C. H. Isolated Metal Atom Geometries as a Strategy for Selective Heterogeneous Hydrogenations. *Science* **2012**, *335*, 1209–1212.
- (14) Boucher, M. B.; Zugic, B.; Cladaras, G.; Kammert, J.; Marcinkowski, M. D.; Lawton, T. J.; Sykes, E. C. H.; Flytzani-Stephanopoulos, M. Single Atom Alloy Surface Analogs in Pd<sub>0.18</sub>Cu<sub>15</sub> Nanoparticles for Selective Hydrogenation Reactions. *Phys. Chem. Chem. Phys.* **2013**, *15*, 12187–12196.
- (15) Lucci, F. R.; Liu, J.; Marcinkowski, M. D.; Yang, M.; Allard, L. F.; Flytzani-Stephanopoulos, M.; Sykes, E. C. H. Selective Hydrogenation of 1,3-Butadiene on Platinum—Copper Alloys at the Single-Atom Limit. *Nat. Commun.* **2015**, *6*, 8550.
- (16) Yang, K.; Yang, B. Identification of the Active and Selective Sites over a Single Pt Atom-Alloyed Cu Catalyst for the Hydrogenation of 1,3-Butadiene: A Combined DFT and Microkinetic Modeling Study. *J. Phys. Chem. C* **2018**, 122, 10883–10891.
- (17) Liu, D.; Chen, H. Y.; Zhang, J. Y.; Huang, J. Y.; Li, Y. M.; Peng, Q. M. Theoretical Investigation of Selective Hydrogenation of 1,3-Butadiene on Pt Doping Cu Nanoparticles. *Appl. Surf. Sci.* **2018**, 456, 59–68.
- (18) Lv, C.-Q.; Liu, J.-H.; Guo, Y.; Wang, G.-C. Selective Hydrogenation of 1,3-Butadiene over Single Pt<sub>1</sub>/Cu(111) Model Catalysts: A DFT Study. *Appl. Surf. Sci.* **2019**, 466, 946–955.
- (19) Cao, Y.; Chen, B.; Guerrero-Sánchez, J.; Lee, I.; Zhou, X.; Takeuchi, N.; Zaera, F. Controlling Selectivity in Unsaturated Aldehyde Hydrogenation Using Single-Site Alloy Catalysts. *ACS Catal.* **2019**, *9*, 9150–9157.

- (20) Cao, Y.; Guerrero-Sańchez, J.; Lee, I.; Zhou, X.; Takeuchi, N.; Zaera, F. Kinetic Study of the Hydrogenation of Unsaturated Aldehydes Promoted by CuPt<sub>x</sub>/SBA-15 Single-Atom Alloy (SAA) Catalysts. *ACS Catal.* **2020**, *10*, 3431–3443.
- (21) Albiter, M. A.; Crooks, R. M.; Zaera, F. Adsorption of Carbon Monoxide on Dendrimer-Encapsulated Platinum Nanoparticles: Liquid Versus Gas Phase. *J. Phys. Chem. Lett.* **2010**, *1*, 38–40.
- (22) Zhu, Y.; Zaera, F. Selectivity in the Catalytic Hydrogenation of Cinnamaldehyde Promoted by Pt/SiO<sub>2</sub> as a Function of Metal Nanoparticle Size. *Catal. Sci. Technol.* **2014**, *4*, 955–962.
- (23) Zaera, F. New Advances in the Use of Infrared Absorption Spectroscopy for the Characterization of Heterogeneous Catalytic Reactions. *Chem. Soc. Rev.* **2014**, *43*, 7624–7663.
- (24) Bouman, M.; Zaera, F. Kinetics of Adsorption of Methyl-cyclopentadienyl Manganese Tricarbonyl on Copper Surfaces and Implications for the Atomic Layer Deposition of Thin Solid Films. *J. Phys. Chem. C* **2016**, *120*, 8232–8239.
- (25) Hicks, R. F.; Kellner, C. S.; Savatsky, B. J.; Hecker, W. C.; Bell, A. T. Design and Construction of a Reactor for in Situ Infrared Studies of Catalytic Reactions. *J. Catal.* **1981**, *71*, 216–218.
- (26) Grunwaldt, J.-D.; Baiker, A. In Situ Spectroscopic Investigation of Heterogeneous Catalysts and Reaction Media at High Pressure. *Phys. Chem. Phys.* **2005**, *7*, 3526–3539.
- (27) Yang, Y.; Disselkamp, R. S.; Szanyi, J.; Peden, C. H. F.; Campbell, C. T.; Goodwin, J. J. G. Design and Operating Characteristics of a Transient Kinetic Analysis Catalysis Reactor System Employing in Situ Transmission Fourier Transform Infrared. *Rev. Sci. Instrum.* 2006, 77, 094104.
- (28) Rasmussen, S. B.; Bañares, M. A.; Bazin, P.; Due-Hansen, J.; Ávila, P.; Daturi, M. Monitoring Catalysts at Work in Their Final Form: Spectroscopic Investigations on a Monolithic Catalyst. *Phys. Chem. Chem. Phys.* **2012**, *14*, 2171–2177.
- (29) Wang, J.; Kispersky, V. F.; Nicholas Delgass, W.; Ribeiro, F. H. Determination of the Au Active Site and Surface Active Species via Operando Transmission FTIR and Isotopic Transient Experiments on 2.3 wt.%  $Au/TiO_2$  for the WGS Reaction. *J. Catal.* **2012**, 289, 171–178
- (30) Carías-Henriquez, A.; Pietrzyk, S.; Dujardin, C. Modelling and Optimization of IR Cell Devoted to in Situ and Operando Characterization of Catalysts. *Catal. Today* **2013**, 205, 134–140.
- (31) Pritchard, J.; Catterick, T.; Gupta, R. K. Infrared Spectroscopy of Chemisorbed Carbon Monoxide on Copper. *Surf. Sci.* **1975**, *S3*, 1–20.
- (32) Kohler, M. A.; Cant, N. W.; Wainwright, M. S.; Trimm, D. L. Infrared Spectroscopic Studies of Carbon Monoxide Adsorbed on a Series of Silica-Supported Copper Catalysts in Different Oxidation States. *J. Catal.* 1989, 117, 188–201.
- (33) Dandekar, A.; Vannice, M. A. Determination of the Dispersion and Surface Oxidation States of Supported Cu Catalysts. *J. Catal.* **1998**, *178*, 621–639.
- (34) Hadjiivanov, K.; Knözinger, H. FTIR Study of CO and NO Adsorption and Coadsorption on a Cu/SiO<sub>2</sub> Catalyst: Probing the Oxidation State of Copper. *Phys. Chem. Chem. Phys.* **2001**, *3*, 1132–1137.
- (35) Nielsen, N. D.; Smitshuysen, T. E. L.; Damsgaard, C. D.; Jensen, A. D.; Christensen, J. M. Characterization of Oxide-Supported Cu by Infrared Measurements on Adsorbed CO. *Surf. Sci.* **2021**, 703, 121725.
- (36) Redhead, P. A. Thermal Desorption of Gases. Vacuum 1962, 12, 203-211.
- (37) Kokalj, A.; Makino, T.; Okada, M. DFT and TPD Study of the Role of Steps in the Adsorption of CO on Copper: Cu(410) Versus Cu(100). *J. Phys.: Condens. Matter* **2017**, *29*, 194001.
- (38) Peterlinz, K. A.; Curtiss, T. J.; Sibener, S. J. Coverage Dependent Desorption Kinetics of CO from Rh(111) Using Time-Resolved Specular Helium Scattering. *J. Chem. Phys.* **1991**, 95, 6972–6985.

- (39) Cardona-Martinez, N.; Dumesic, J.A. Applications of Adsorption Microcalorimetry to the Study of Heterogeneous Catalysis. *Adv. Catal.* **1992**, *38*, 149–244.
- (40) Savara, A. Standard States for Adsorption on Solid Surfaces: 2d Gases, Surface Liquids, and Langmuir Adsorbates. *J. Phys. Chem. C* **2013**, *117*, 15710–15715.
- (41) Pritchard, J.; Catterick, T. Infrared Spectroscopy. In Experimental Methods in Catalytic Research; Anderson, R. B., Dawson, P. T., Eds.; Academic Press: New York, 1976; Vol. III, pp 281–318
- (42) Sheppard, N.; Nguyen, T. T. Chapter 2: The Vibrationa Spectra of Carbon Monoxide Chemisorbed on the Surfaces of Metal Catalysts A Suggested Scheme of Interpretation. *Adv. Infrared Raman Spectrosc.* **1978**, *5*, 67–148.
- (43) Hoffmann, F. M. Infrared Reflection-Absorption Spectroscopy of Adsorbed Molecules. Surf. Sci. Rep. 1983, 3, 107–192.
- (44) Stacchiola, D. J. Tuning the Properties of Copper-Based Catalysts Based on Molecular in Situ Studies of Model Systems. *Acc. Chem. Res.* **2015**, *48*, 2151–2158.
- (45) Raval, R.; Parker, S. F.; Pemble, M. E.; Hollins, P.; Pritchard, J.; Chesters, M. A. FT-RAIRS, EELS and LEED Studies of the Adsorption of Carbon Monoxide on Cu(111). *Surf. Sci.* **1988**, 203, 353–377.
- (46) Wadayama, T.; Kubo, K.; Yamashita, T.; Tanabe, T.; Hatta, A. Infrared Reflection Absorption Study of Carbon Monoxide Adsorbed on Submonolayer Fe-Covered Cu(100), (110), and (111) Bimetallic Surfaces. J. Phys. Chem. B 2003, 107, 3768–3773.
- (47) Mudiyanselage, K.; An, W.; Yang, F.; Liu, P.; Stacchiola, D. J. Selective Molecular Adsorption in Sub-Nanometer Cages of a Cu<sub>2</sub>O Surface Oxide. *Phys. Chem. Chem. Phys.* **2013**, *15*, 10726–10731.
- (48) Kruppe, C. M.; Krooswyk, J. D.; Trenary, M. Polarization-Dependent Infrared Spectroscopy of Adsorbed Carbon Monoxide to Probe the Surface of a Pd/Cu(111) Single-Atom Alloy. *J. Phys. Chem.* C 2017, 121, 9361–9369.
- (49) Hollins, P.; Pritchard, J. Interactions of CO Molecules Adsorbed on Oxidised Cu(111) and Cu(110). Surf. Sci. 1983, 134, 91–108.
- (50) Borguet, E.; Dai, H.-L. Site-Specific Properties and Dynamic Dipole Coupling of CO Molecules Adsorbed on a Vicinal Cu(100) Surface. *J. Chem. Phys.* **1994**, *101*, 9080–9095.
- (51) Kavtaradze, N. N.; Sokolova, N. P. A Study of the Infrared Spectra of Carbon Monoxide Adsorbed on Metals of the Copper Subgroup and on Cobalt, Ruthenium, Rhodium, and Palladium. *J. Appl. Spectrosc.* **1966**, *4*, 325–330.
- (\$2) Padley, M. B.; Rochester, C. H.; Hutchings, G. J.; King, F. FTIR Spectroscopic Study of Thiophene, SO<sub>2</sub>, and CO Adsorption on Cu/Al<sub>2</sub>O<sub>3</sub> Catalysts. *J. Catal.* **1994**, *148*, 438–452.
- (53) Hollins, P.; Pritchard, J. Interactions of CO Molecules Adsorbed on Cu(111). Surf. Sci. 1979, 89, 486-495.
- (54) Harendt, C.; Goschnick, J.; Hirschwald, W. The Interaction of CO with Copper (110) Studied by TDS and LEED. *Surf. Sci.* **1985**, 152, 453–462.
- (55) Simonovis, J. P.; Hunt, A.; Palomino, R. M.; Senanayake, S. D.; Waluyo, I. Enhanced Stability of Pt-Cu Single-Atom Alloy Catalysts: In Situ Characterization of the Pt/Cu(111) Surface in an Ambient Pressure of CO. *J. Phys. Chem. C* **2018**, *122*, 4488–4495.
- (56) Clayton, J. O.; Giauque, W. F. The Heat Capacity and Entropy of Carbon Monoxide. Heat of Vaporization. Vapor Pressures of Solid and Liquid. Free Energy to 5000 K. From Spectroscopic Data. *J. Am. Chem. Soc.* **1932**, *54*, 2610–2626.
- (57) Savara, A.; Schmidt, C. M.; Geiger, F. M.; Weitz, E. Adsorption Entropies and Enthalpies and Their Implications for Adsorbate Dynamics. *J. Phys. Chem. C* **2009**, *113*, 2806–2815.
- (58) Yates, J. T., Jr.; Goodman, D. W. Carbon Monoxide Chemisorption on Ni(100) Direct Detection of Adsorbate-Adsorbate Interactions by Desorption Kinetic Measurements. *J. Chem. Phys.* **1980**, *73*, 5371–5375.

- (59) Gland, J. L.; Fischer, D. A.; Shen, S.; Zaera, F. Displacement of CO Chemisorbed on Metals by Hydrogen. *J. Am. Chem. Soc.* **1990**, 112, 5695.
- (60) Kash, P. W.; Yang, M. X.; Teplyakov, A. V.; Flynn, G. W.; Bent, B. E. Chemical Displacement of Molecules Adsorbed on Copper Surfaces: Low-Temperature Studies with Applications to Surface Reactions. *J. Phys. Chem. B* **1997**, *101*, 7908–7918.
- (61) Bowker, M.; King, D. A. Anomalous Adsorption Kinetics. Γ-Nitrogen on the {110} Plane of Tungsten. *J. Chem. Soc. Faraday Trans.* 1 1979, 75, 2100–2115.
- (62) Arumainayagam, C. R.; McMaster, M. C.; Madix, R. J. Coverage Dependence of Molecular Adsorption Dynamics: Ethane on Platinum (111). *J. Phys. Chem.* **1991**, *95*, 2461–2465.
- (63) Molinari, E.; Tomellini, M. Role of Vibrational Excitation of the Adlayer in 'Precursor-Mediated' Sticking Probabilities of CO on Metal Surfaces: A Kinetic Model. Z. Phys. Chem. (Munich) 2012, 226, 253–274.
- (64) Karakalos, S.; Lawton, T. J.; Lucci, F. R.; Sykes, E. C. H.; Zaera, F. Enantiospecific Kinetics in Surface Adsorption: Propylene Oxide on Pt(111) Surfaces. *J. Phys. Chem. C* **2013**, *117*, 18588–18594.
- (65) Peacock-López, E.; Suhl, H. Compensation Effect in Thermally Activated Processes. *Phys. Rev. B* **1982**, *26*, 3774.
- (66) Bond, G. C.; Keane, M. A.; Kral, H.; Lercher, J. A. Compensation Phenomena in Heterogeneous Catalysis: General Principles and a Possible Explanation. *Catal. Rev.-Sci. Technol.* **2000**, 42, 323–383.
- (67) Liu, L.; Guo, Q.-X. Isokinetic Relationship, Isoequilibrium Relationship, and Enthalpy–Entropy Compensation. *Chem. Rev.* **2001**, *101*, *673*–*696*.
- (68) Bligaard, T.; Honkala, K.; Logadottir, A.; Nørskov, J. K.; Dahl, S.; Jacobsen, C. J. H. On the Compensation Effect in Heterogeneous Catalysis. *J. Phys. Chem. B* **2003**, *107*, 9325–9331.

